Electrochimica Acta 68 (2012) 153–157

Contents lists available at SciVerse ScienceDirect

Electrochimica Acta

journal homepage: www.elsevier.com/locate/electacta

Improved electrochemical performances of $LiM_{0.05}Co_{0.95}O_{1.95}F_{0.05}$ (M = Mg, Al, Zr) at high voltage

Hun-Gi Jung[a,c], Nulu Venu Gopal[a], Jai Prakash[b], Dong-Won Kim[c], Yang-Kook Sun[a,c,*]

[a] Department of WCU Energy Engineering, Hanyang University, Seoul 133-791, South Korea
[b] Department of Chemical and Environmental Engineering, Illinois Institute of Technology, IL 60616, USA
[c] Department of Chemical Engineering, Hanyang University, Seoul 133-791, South Korea

ARTICLE INFO

Article history:
Received 28 August 2011
Received in revised form 19 January 2012
Accepted 12 February 2012
Available online 24 February 2012

Keywords:
Cathode material
Lithium batteries
Metal and fluorine substitution
High voltage

ABSTRACT

Metal and F co-substituted $LiM_{0.05}Co_{0.95}O_{1.95}F_{0.05}$ (M = Mg, Al, Zr) cathode materials were successfully synthesized via a solid-state reaction. XRD measurements showed that cobalt and oxygen sites in $LiCoO_2$ are successfully substituted for metal (Mg, Al, Zr) and fluorine, respectively. The co-substituted materials exhibited stable cycling performance, improved rate capability, and thermal stability compared to pristine $LiCoO_2$. Furthermore, Co dissolution tests revealed that fluorine substitution stabilizes the cathode surface and thus suppresses Co dissolution. Among the materials, $LiMg_{0.05}Co_{0.95}O_{1.95}F_{0.05}$ showed the best electrochemical and thermal properties.

1. Introduction

Li-ion batteries (LIB) are becoming the most important power sources for portable electronic devices due to their high energy density and excellent cycling stability. In the next few years, an ever-increasing demand for portable electronic devices will require high performance rechargeable batteries with high energy and power densities. Currently, the most commonly used cathode material for Li-ion batteries is $LiCoO_2$ due to its high capacity, excellent cycle life, good rate capability, and high energy density. Though $LiCoO_2$ has a theoretical capacity of 274 mAh g^{-1}, it only delivers a reversible capacity of 140 mAh g^{-1} when charged to 4.2 V vs. Li/Li^+. In order to improve the discharge capacity of $LiCoO_2$, an upper cutoff voltage above 4.2 V must be applied to extract more Li^+ in $LiCoO_2$, but this causes severe capacity fading. The reason for the poor cycling performance above 4.2 V is structural instability caused by the phase transition from the hexagonal to monoclinic phase accompanied by a 1.2% crystal lattice expansion along the *c* direction [1–3]. In addition, Co dissolution coupled with the phase change results in capacity loss of $LiCoO_2$ at cutoff voltages higher than 4.5 V [3].

To overcome these problems, cathode particle surfaces were modified with metal oxides [4–6]. Cho et al. [4] reported that Al_2O_3 and ZrO_2-coated $LiCoO_2$ powders delivered a capacity of more than 170 mAh g^{-1} with an excellent cycling stability in the voltage range between 2.7 and 4.4 V and hypothesized that thin-film coating of the high fracture toughness oxide of ZrO_2 on $LiCoO_2$, a so-called zero-strain material, stabilized the hexagonal symmetry during delithiation, and thereby suppressed the phase transitions. However, Chen and Dahn [7,8] reported that the excellent capacity retention of $LiCoO_2$ coated with metal oxides (ZrO_2, Al_2O_3, and SiO_2) charged to 4.5 V was not due to an increase in fracture toughness of the coated oxide but rather to the suppression of side reactions between the cathode and the electrolyte. We also verified that an amphoteric metal oxide coating layer acting as a HF scavenger converted to metal fluoride during cycling in previous studies [9–11]. These findings suggest that the metal oxide coating layer is not immune to HF attack in the electrolyte. Therefore, AlF_3 has been proposed to be a new coating material and has showed greatly enhanced electrochemical performance for all cathode materials as compared to the corresponding pristine materials at a high cutoff voltage [12–16]. The improved electrochemical performance with the AlF_3 coating on $LiCoO_2$ was attributed to the lowered charge-transfer resistance caused by the suppression of Co dissolution, which effectively delays the eventual phase transformation to a spinel phase during cycling; this conclusion was confirmed by Co dissolution data along with TEM analysis [17].

Reports on partial substitution of cobalt in $LiCoO_2$ by Al, Mg and Zr [18–22] have suggested that the substitution effect prevents

* Corresponding author at: Department of WCU Energy Engineering, Hanyang University, Seoul 133-791, South Korea. Tel.: +82 2 2220 0524; fax: +82 2 2282 7329.
E-mail address: yksun@hanyang.ac.kr (Y.-K. Sun).

0013-4686/$ – see front matter © 2012 Elsevier Ltd. All rights reserved.
doi:10.1016/j.electacta.2012.02.057

overcharging and volume changes in the cathode material during cycling. Jang et al. [2] reported that doping with Al in $LiCoO_2$ ($LiAl_yCo_{1-y}O_2$; $y = 0.25–0.5$) facilitates the initial discharge capacity but shows rapid capacity fading when cycled at 4.5 V up to 10 cycles. Zou et al. [21] demonstrated that doping $LiCoO_2$ with Bi, Cr, Sn and Zr significantly improves the discharge capacity at 0.2 C-rate when cycled between 3 and 4.5 V. Fluorine substitution for oxygen up to a certain level in $Li[Ni_{0.8}Co_{0.1}Mn_{0.1}]O_{2-z}F_z$ significantly improved the cyclability (3.0–4.3 V) compared to pristine $Li[Ni_{0.8}Co_{0.1}Mn_{0.1}]O_2$, due to fluorine substitution on the surface, which acts as a protecting layer against HF in the electrolyte during cycling [23]. However, it is still a great challenge for researchers to develop a cathode material with high specific capacity and good cycling stability at higher voltages (4.5 V).

In this report, we studied the combined effects of metal (Al, Mg, and Zr) substitution for Co and F for O in $LiCoO_2$ on the electrochemical performance at a higher cutoff voltage of 4.5 V.

2. Experimental

$LiCoO_2$ was prepared by a solid-state reaction method. Stoichiometric amounts of Co_3O_4 (99.9%) and Li_2CO_3 (>99.9%) were thoroughly mixed and calcined at 850 °C for 20 h in air. $LiM_{0.05}Co_{0.95}O_{1.95}F_{0.05}$ (M = Mg, Al, Zr, hereafter LMCOF) powders were prepared using the same procedure as for $LiCoO_2$ but also using different doping agents: MgF_2 and $Mg(OH)_2$ for $LiMg_{0.05}Co_{0.95}O_{1.95}F_{0.05}$, AlF_3 and $Al(OH)_3$ for $LiAl_{0.05}Co_{0.95}O_{1.95}F_{0.05}$, and ZrF_4 and ZrO_2 for $LiZr_{0.05}Co_{0.95}O_{1.95}F_{0.05}$. The Mg-substituted $LiMg_{0.05}Co_{0.95}O_{1.95}F_{0.05}$, Al-substituted $LiAl_{0.05}Co_{0.95}O_{1.95}F_{0.05}$, and Zr-substituted $LiZr_{0.05}Co_{0.95}O_{1.95}F_{0.05}$ materials are hereafter referred to as LMgCOF, LAlCOF, and LZrCOF, respectively.

The phase purity of the prepared powders was characterized by powder X-ray diffraction (XRD) using Cu Kα radiation (Rint-2000, Rigaku). Lattice parameters were calculated by a least-squares method from the XRD patterns. The morphologies and distributions of the prepared powders were also observed using scanning electron microscopy (SEM, JSM-6340F, JEOL). To measure the dissolved amount of Co, coin-type half-cells containing pristine $LiCoO_2$ and LMCOF charged to 4.5 V were carefully disassembled in a glove box. The recovered cathode active materials were stored in electrolyte at 60 °C, and the amount of Co dissolution into electrolyte with storage time was measured by atomic absorption spectroscopy (AAS) (Analytik Jena AG, Vario 6). Thermal investigations of fully charged cathode were carried out using a differential scanning calorimeter (DSC) (NETZSCH-TA4) at a temperature scan rate of 5 °C min^{-1} in the temperature range of 100–350 °C.

Electrochemical properties of the prepared powders were evaluated with coin-type half-cells (CR2032). The cathode was fabricated with a mixture of 85 wt.% of the prepared powder, 7.5 wt.% carbon black, and 7.5 wt.% poly(vinylidene difluoride) binder on an aluminum current collector. The anode was lithium metal. Cells were constructed with the electrodes separated by a porous polypropylene film. The electrolyte was a 1:1 mixture of ethylene carbonate (EC) and diethyl carbonate (DEC) containing 1M $LiPF_6$ by volume (PANAX ETEC Co. Ltd).

3. Results and discussion

Fig. 1 shows the XRD patterns of the pristine $LiCoO_2$ and LMCOF powders. All peaks were indexed based on a hexagonal α-$NaFeO_2$ structure with a space group of $R\bar{3}m$ (JCPDS card no. 44-145), indicating that partial metal and fluorine substitution did not change the hexagonal layer structure. The clear split of the (0 0 6)/(1 0 2) and (1 0 8)/(1 1 0) doublets for all samples indicates the formation

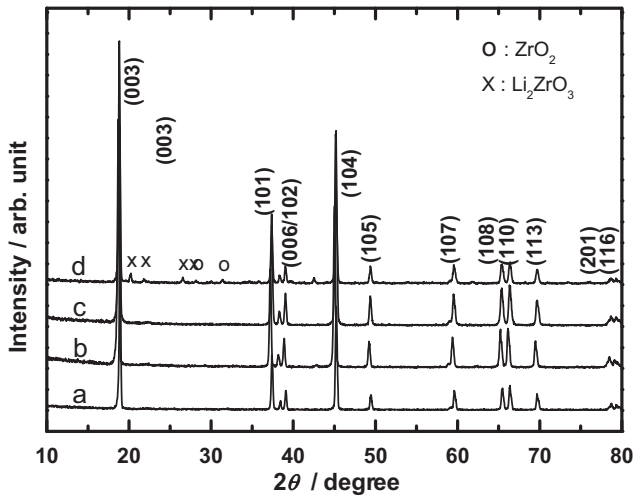

Fig. 1. Powder XRD patterns of (a) pristine $LiCoO_2$, (b) LMgCOF, (c) LAlCOF, and (d) LZrCOF.

of a well-ordered layer structure. However, impurity peaks of ZrO_2 at $2\theta = 28°$ and 32°, and Li_2ZrO_3 at $2\theta = 21°$, 23°, 26°, and 43° are observed for LZrCOF powder, as shown in Fig. 1d.

Variation in lattice parameters, *a* and *c*, and *c*/*a* ratio values for pristine $LiCoO_2$ and LMCOF are given in Fig. 2. The increases in both axes for the LMCOF could be due to the incorporation of substitution elements into the crystal structure. Among all the substituted $LiCoO_2$ samples, it is clear that the partial substitution of cobalt and oxygen ions by Mg and F results in larger "*a*" and shorter "*c*" parameters than the LAlCOF or LZrCOF samples. Kim et al. [19] and Castro-Garcia et al. [20] reported that the substitution of cobalt by the larger Mg^{2+} ion ($r_{Mg^{2+}} = 0.72$ Å) in $LiCoO_2$ decreases the thickness of the CoO_2 slab, thus resulting in an increase in the inter slab distance. However, the incorporation with the smaller and more polarizable Al^{3+} ion ($r_{Al^{3+}} = 0.57$ Å) tends to distort the structure and increase the interlayer distance along the c-axis due to an increase in coulomb repulsion within the [CoO_2] layers [20]. Although Zr^{4+} ($r_{Zr^{4+}} = 0.72$ Å) has an ionic radius similar to that of Mg^{2+}, it shows a smaller "*a*" parameter value than the LMgCOF. This is presumably because the doping concentration of Zr^{4+} is limited in its ability to make a solid solution with $LiCoO_2$ [22]; excess Zr^{4+} may produce ZrO_2 along with secondary phase formation of Li_2ZrO_3 as impurities. In this context, the increase in lattice constants along the *a* and *c*-axis compared to pristine $LiCoO_2$ gives evidence that metal and fluorine ions are successfully substituted for cobalt and oxygen

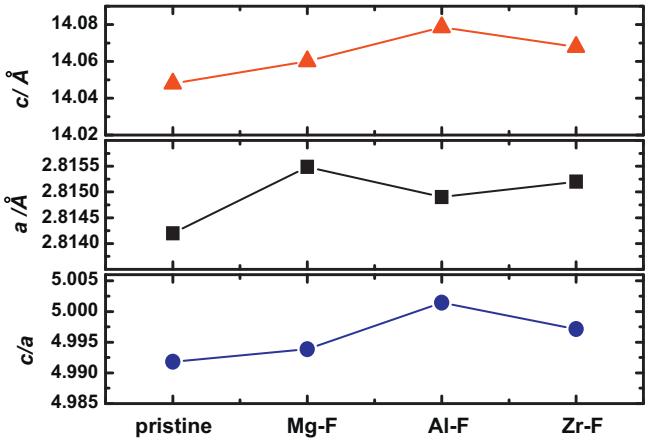

Fig. 2. Lattice parameters of pristine $LiCoO_2$, LMgCOF, LAlCOF, and LZrCOF.

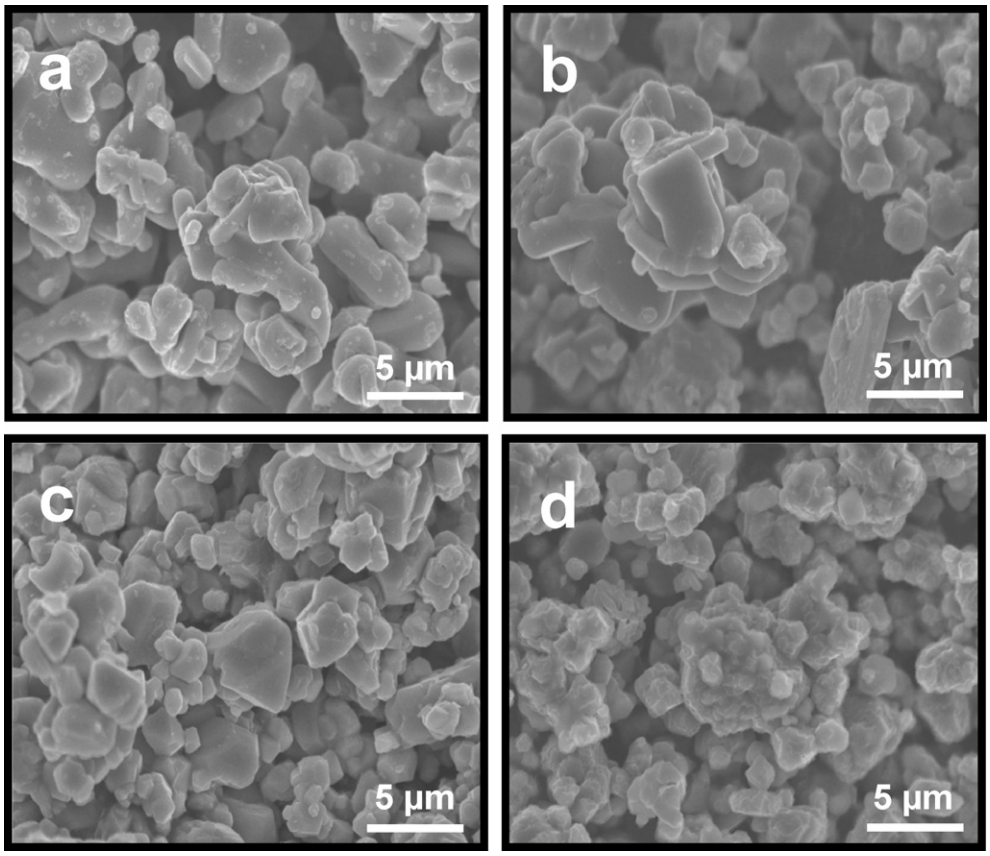

Fig. 3. SEM images of (a) pristine $LiCoO_2$, (b) LMgCOF, (c) LAlCOF, and (d) LZrCOF.

sites, respectively, in the layered hexagonal structure with no further generation of secondary phases [24]. As shown in Fig. 2, the LMgCOF, LAlCOF, and LZrCOF samples show greater variation in *c*/*a* values of 4.994, 5.002 and 4.997 than the pristine $LiCoO_2$, indicating that substitution induces the elongation of the hexagonal cell along the *c*-axis, which facilitates more lithium intercalation in 3*a* sites. Similar results were also observed in previous reports on Mg and Zr-doped $LiCoO_2$ [19,22]. Furthermore, it is clear that the *c*/*a* ratio of LMgCOF is smaller than the other samples, reflecting that the degree of trigonal distortion is relatively low.

Fig. 3 shows a SEM image of the pristine $LiCoO_2$, LMgCOF, LAlCOF, and LZrCOF samples. All samples consist of micron-sized particles with size ranges of 1–6 μm. The pristine $LiCoO_2$ and LMgCOF have pillar-like shapes with particle sizes of 3–6 μm while the LAlCOF and LZrCOF exhibit mixed morphologies with slightly smaller particle sizes. As expected, this kind of irregular morphology reduces the electrochemical properties.

Fig. 4a shows the initial charge–discharge curves for Li/pristine $LiCoO_2$ and Li/LMCOF cells at a constant current density of 32 mA g^{-1} (0.2 C-rate) in a potential range of 3.0–4.5 V. All cells exhibited smooth charge–discharge curves and had typical phase transition peaks at around 4.2 V. Pristine $LiCoO_2$ delivered similar discharge capacity (184 mAh g^{-1}) and voltage-capacity profiles as previously reported results on $LiCoO_2$ [25]. However, among the samples, LZrCOF delivered the lowest initial discharge capacity due to the presence of some impurity phases and irregular surface morphology (as shown in Fig. 3d). On the other hand, the LMgCOF exhibited the highest initial discharge capacity of around 185 mAh g^{-1} compared to LMCOF (M = Al, Zr). Tukamoto and West [26] reported similar electrochemical behavior in Mg-substituted $LiCoO_2$, which is ascribed to the increase in electronic conductivity of the host structure caused by the generation of holes within

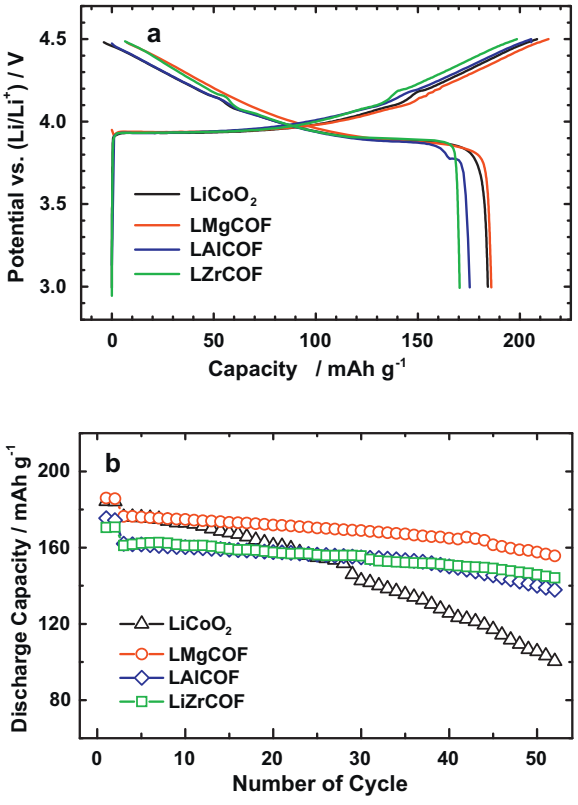

Fig. 4. (a) Initial charge–discharge curves of Li/pristine $LiCoO_2$, LMgCOF, LAlCOF, and LZrCOF cells; applied current density was 32 mA g^{-1} (0.2 C-rate) between 3.0 and 4.5 V. (b) Corresponding cycling performance at a current density of 80 mA g^{-1} (0.5 C-rate).

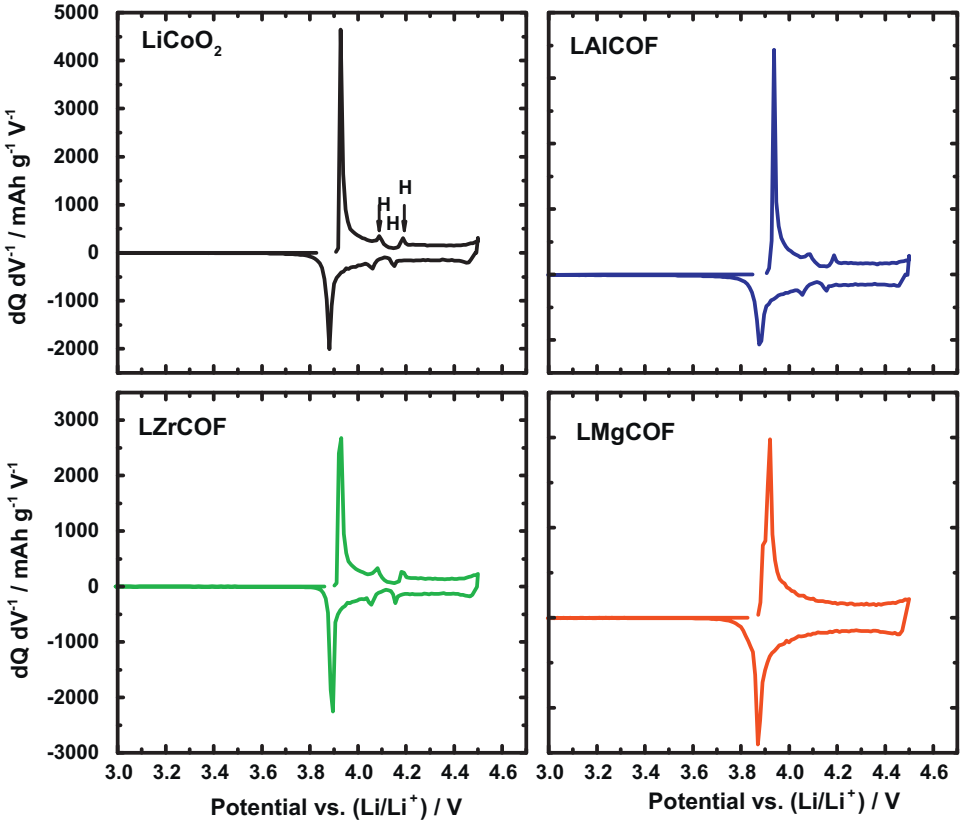

Fig. 5. $dQ\,dV^{-1}$ vs. V curves of Li/pristine $LiCoO_2$, LMgCOF, LAlCOF, and LZrCOF cells observed during the first cycle at a 32 mA g^{-1} (0.2 C-rate) between 3.0 and 4.5 V.

the solid solution. In addition, as discussed earlier (Fig. 3a and b), the well-crystallized microstructures (average grain size of about more than 2 μm) of LMgCOF would be much helpful to achieve higher initial discharge capacity values than the other samples.

Fig. 4b shows the cycling performance of pristine $LiCoO_2$ and LMCOF samples. Tests were conducted in the voltage range of 3.0–4.5 V at a 0.5 C-rate (80 mA g^{-1}) after 2 cycles at 0.2 C-rate. The pristine $LiCoO_2$ shows very poor cyclability with only 61% capacity retention after 50 cycles. In contrast, the LMgCOF exhibits slightly higher initial discharge capacity and more enhanced cycle performance than the pristine $LiCoO_2$. Cells employing LAlCOF and LZrCOF show lower initial discharge capacities than the pristine $LiCoO_2$, but they exhibit significant capacity retention. Another reason for the improved cycling performance of LMCOF electrode is F substitution for O site by stabilization of cathode surface caused by stronger metal-fluorine bonding than metal-oxygen bonding. The enhanced cycling performance was observed in the $Li[Ni_{1/3}Co_{1/3}Mn_{1/3}]O_{2-z}F_z$ ($z = 0.05$) cycled to 4.6 V [24]. We believe that substitution of F for O reduces the interfacial resistance between cathode and the electrolyte, and acts as a protecting layer on the cathode surface against HF attack in the electrolyte during extended cycling.

Fig. 5 shows the differential capacity (dQ/dV) vs. voltage profiles of Li/pristine $LiCoO_2$ and Li/LMCOF cells for the first cycle. All cells exhibited charging peaks at around 3.92 V and discharge peaks at around 3.88 V, which are attributed to the phase transition between two O3 structures [27]. It is clearly observed that, except LMgCOF, all cells show redox peaks at around 4.1 V and 4.2 V, indicating that doping with Al-F and Zr-F cannot prevent phase transition (hexagonal to monoclinic) of $LiCoO_2$ during electrochemical cycling. However, Mg-F substitution suppressed the phase transition and hence improved the structural stability of the host structure by minimizing the strain within the slabs of cobalt oxide.

Fig. 6 shows the rate capabilities of Li/pristine $LiCoO_2$ and Li/LMCOF cells at various current rates between 3.0 and 4.5 V. All the cells were charged at a current density of 32 mA g^{-1} (0.2 C-rate) and then discharged at different current densities 32 mA g^{-1} (0.2 C-rate) to 480 mA g^{-1} (3 C-rate). The capacity retention for pristine $LiCoO_2$ decreases drastically with an increase in discharge rate, especially at higher discharge current rates. In contrast, LMCOF electrodes showed less variation in capacity fading even at higher discharge rates. Similar to cycling behavior, LMgCOF electrodes showed the best rate characteristics, i.e., 85% capacity retention at a 3 C-rate.

Our group [17] and Amatucci et al. [3] reported that the capacity fading of $LiCoO_2$ at higher voltage is directly related to the amount of Co dissolution during cycling. Fig. 7 plots the measured amounts of cobalt dissolution from the pristine $LiCoO_2$ and LMCOF samples

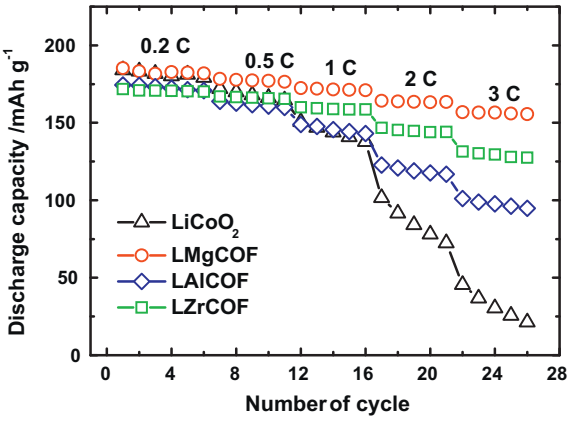

Fig. 6. Rate capability of the Li/pristine $LiCoO_2$, LMgCOF, LAlCOF, and LZrCOF cells cycled between 3.0 and 4.5 V at various C rates.

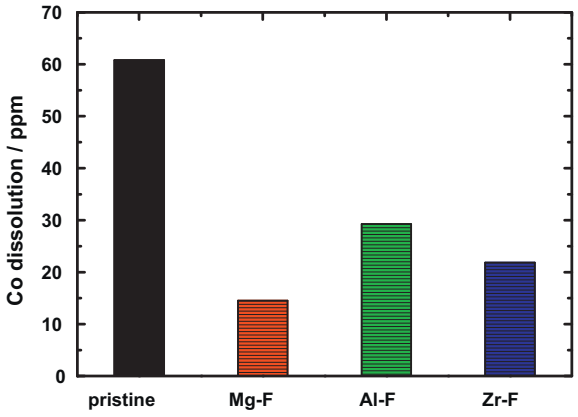

Fig. 7. Amount of Co dissolution of the pristine $LiCoO_2$, LMgCOF, LAlCOF, and LZrCOF samples after 7 days storage at 60 °C.

after 7 days of storage at 60 °C. The Co dissolution from the LMCOF was substantially suppressed compared with the pristine $LiCoO_2$, which was consistent with the capacity loss shown in Fig. 4. LMgCOF shows the lowest cobalt dissolution of all the samples. Another reason for the reduced Co dissolution in LMCOF is that F substitution can effectively minimize chemical reactions occurring on the electrode surface at cutoff voltages higher than 4.5 V [23,24]. Therefore, the synergetic effect of dual ion substituents into the $LiCoO_2$ structure improves the structural stability, capacity retention, and rate capability of $LiCoO_2$ at high cutoff voltages.

Fig. 8 exhibits the DSC profiles of pristine $LiCoO_2$ and LMCOF, which were charged to 4.5 V. Pristine $LiCoO_2$ had an exothermic peak at 232.7 °C with an onset temperature of 155 °C and heat generation of 2418 J g^{-1}. All the LMCOF electrodes showed improved thermal stability compared to pristine $LiCoO_2$; the exothermic peak and onset temperature are 256 °C and 201 °C for LMgCOF, 244 °C and 201 °C for LAlCOF, and 243 °C and 166 °C for LZrCOF, respectively. Even though equal amounts of fluorine were substituted in all the substituted electrodes, they showed variations in thermal behavior. This indicates that the thermal stability is mostly affected by the cation-type, i.e., among the Mg, Zr and Al ions, especially, substitution with Mg significantly increases the structural stability of the layered structure [19,22]. Further, substitution with fluorine also substantially increases the thermal stability of layered LMCOF structure by improving its structural stability, which is in accordance with our previous report on fluorine substituted

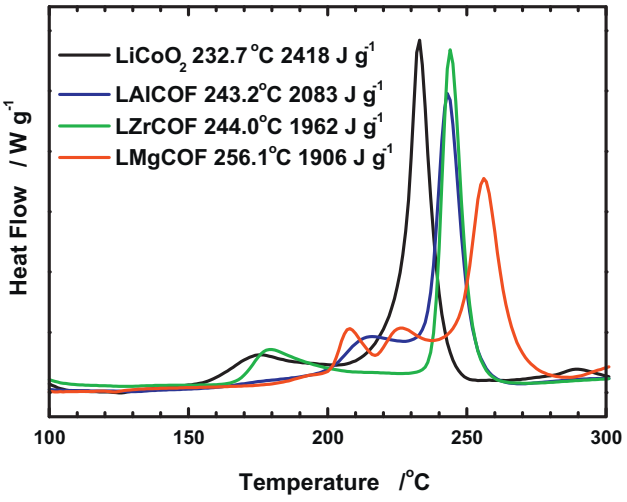

Fig. 8. DSC traces of delithiated pristine $LiCoO_2$, LMgCOF, LAlCOF, and LZrCOF electrodes charged to 4.5 V.

layered $Li[Ni_{0.8}Co_{0.1}Mn_{0.1}]O_2$ cathode material [23]. Thus, when Mg-F is substituted, thermal stability of the host structure is greatly improved, resulting in the highest exothermic peak temperature and the lowest heat generation (1906 J g^{-1}).

4. Conclusions

We synthesized metal (Mg, Al, and Zr) and fluorine co-substituted $LiM_{0.05}Co_{0.95}O_{1.95}F_{0.05}$ (M = Mg, Al, Zr) by solid-state reactions. Metal ion substitution for Co site increases the inter slab distance in $LiCoO_2$ (a parameter) which promotes Li^+ diffusion while substitution with fluorine for O site protects the cathode surface against HF attack in electrolyte, thereby reducing Co dissolution. Therefore, metal and F co-substituted materials show enhanced electrochemical and thermal properties at higher cutoff voltages of 4.5 V, compared to pristine material. $LiMg_{0.05}Co_{0.95}O_{1.95}F_{0.05}$ exhibits the highest initial capacity of 185 mAh g^{-1}, excellent rate capability of 156 mAh g^{-1} at a 3 C-rate and cycling performance with capacity retention of 88% after 50 cycles (0.5 C-rate).

Acknowledgements

This work was supported by the Human Resources Development of the Korea Institute of Energy Technology Evaluation and Planning (KETEP) grant funded by the Korea government Ministry of Knowledge Economy (No. 20104010100560), and by the WCU (World Class University) program through the Korea Science and Engineering Foundation by Education, Science, and Technology (R31-2008-000-10092).

References

[1] T. Ohzuku, A. Ueda, J. Electrochem. Soc. 141 (1994) 2972.
[2] Y. Jang, B. Huang, H. Wang, G.-R. Maskaly, G. Ceder, D.-R. Sadoway, Y.-M. Chiang, H. Liu, H. Tamura, J. Power Sources 81–82 (1999) 589.
[3] G.G. Amatucci, J.M. Tarascon, L.C. Klein, Solid State Ionics 83 (1996) 167.
[4] J. Cho, Y.J. Kim, T.-J. Kim, B. Park, Angew. Chem. Int. Ed. 40 (2001) 3367.
[5] Y.-K. Sun, Y.-S. Lee, M. Yoshio, K. Amine, Electrochem. Solid State Lett. 5 (2002) A99.
[6] S.-T. Myung, K. Izumi, S. Komaba, H. Yashiro, H.J. Bang, Y.-K. Sun, N. Kumagai, J. Phys. Chem. C 111 (2007) 4061.
[7] Z. Chen, J.R. Dahn, Electrochem. Solid State Lett. 6 (2003) A221.
[8] Z. Chen, J.R. Dahn, Electrochim. Acta 49 (2004) 1079.
[9] Y.-K. Sun, K.-J. Hong, J. Prakash, K. Amine, Electrochem. Commun. 4 (2002) 344.
[10] S.-T. Myung, K. Izumi, S. Komaba, Y.-K. Sun, H. Yashiro, N. Kumagai, Chem. Mater. 17 (2005) 3695.
[11] J.-M. Han, S.-T. Myung, Y.-K. Sun, J. Electrochem. Soc. 153 (2006) A1290.
[12] Y.-K. Sun, J.-M. Han, S.-T. Myung, S.-W. Lee, K. Amine, Electrochem. Commun. 8 (2006) 821.
[13] Y.-K. Sun, S.-W. Cho, S.-W. Lee, C.S. Yoon, K. Amine, J. Electrochem. Soc. 154 (2007) A168.
[14] S.-U. Woo, C.S. Yoon, K. Amine, I. Belharouak, Y.-K. Sun, J. Electrochem. Soc. 154 (2007) A1005.
[15] H.-B. Kim, B.-C. Park, S.-T. Myung, K. Amine, J. Prakash, Y.-K. Sun, J. Power Sources 179 (2008) 347.
[16] Y.-K. Sun, S.-T. Myung, B.-C. Park, H. Yashiro, J. Electrochem. Soc. 155 (2008) A705.
[17] Y.-K. Sun, C.S. Yoon, S.-T. Myung, I. Belharouak, K. Amine, J. Electrochem. Soc. 156 (2009) A1005.
[18] Y.-I. Jang, B. Huang, D.R. Sadoway, G. Ceder, Y.-M. Chiang, H. Lui, H. Tamura, J. Electrochem. Soc. 146 (1999) 862.
[19] H.-J. Kim, Y.U. Jeong, J.-H. Lee, J.-J. Kim, J. Power Sources 159 (2006) 233.
[20] S. Castro-García, A. Castro-Couceiro, M.A. Señarís-Rodríguez, F. Soulette, C. Julien, Solid State Ionics 156 (2003) 15.
[21] M. Zou, M. Yoshio, S. Gopukumar, J. Yamaki, Chem. Mater. 17 (2005) 1284.
[22] H.-S. Kim, T.-K. Ko, B.-K. Na, W.I. Cho, B.W. Cho, J. Power Sources 138 (2004) 232.
[23] S.-U. Woo, B.-C. Park, C.S. Yoon, S.-T. Myung, J. Prakash, Y.-K. Sun, J. Electrochem. Soc. 154 (2007) A649.
[24] G.-H. Kim, J.-H. Kim, S.-T. Myung, C.S. Yoon, Y.-K. Sun, J. Electrochem. Soc. 152 (2005) A1707.
[25] Y.-K. Sun, S.-W. Cho, S.-T. Myung, K. Amine, J. Prakash, Electrochim. Acta 53 (2007) 1013.
[26] H. Tukamoto, A.R. West, J. Electrochem. Soc. 144 (1997) 3164.
[27] A.-V. Ven, G. Ceder, Electrochem, Solid State Lett. 3 (2000) 301.